AIAA JOURNAL
Vol. 30, No. 2, February 1992

High Reynolds Number Flows in Rotating and Nutating Cylinders: Spatial Eigenvalue Approach

Philip Hall*
University of Manchester, Manchester M1-39-PL, England, United Kingdom
and
Raymond Sedney† and Nathan Gerber‡
U.S. Army Ballistic Research Laboratory, Aberdeen Proving Ground, Maryland 21005

The spatial eigenvalue expansion procedure that we have used previously to study viscous flow in rotating and nutating cylinders is studied in the high Reynolds number limit. It is shown that in this limit there is a significant simplification in the procedure employed to determine the amplitudes of the eigenfunctions used to describe the forced velocity field in the cylinder. More precisely, it is shown that these amplitudes can, to the order of Reynolds number used in this paper, be simply expressed in terms of Bessel functions. The method is used to calculate the pressure coefficient at a point on the end wall. Detailed comparisons with experimental results are made. It is found that the approach provides an accurate and extremely rapid way of determining this pressure coefficient.

I. Introduction and Formulation

IT is well known that there can be a significant difference in behavior in flight between liquid-filled and solid-filled projectiles. The difference is caused by the motion of the liquid inside the spinning projectile. This motion causes forces to act on the projectile that can ultimately cause the flight of the projectile to be prematurely terminated by instability. The initial motion of the projectile necessarily causes the fluid motion in the cylinder to be time dependent; later it can be assumed that the flow is steady. It is the latter situation that is investigated here.

Our concern then is with the motion of an incompressible viscous fluid of kinematic viscosity ν in a cylinder of length $2Aa$ and radius a. The cylinder is spinning at a constant rate about its axis, which, in turn, is nutating at a constant rate and yaw angle about an axis directed along its trajectory. Throughout this calculation, a is used as an appropriate length scale and the magnitude of a typical velocity is taken to be $(\Omega + \bar{\tau} \cos K_0)a$, where Ω is the magnitude of the angular velocity of the projectile as observed in the aeroballistic reference frame, $\bar{\tau}$ is the dimensional coning frequency, and K_0 is the coning angle. (In the aeroballistic frame, one Cartesian coordinate lies along the cylinder axis and a second coordinate lies in the plane of the cylinder axis and trajectory; see, e.g., Ref. 1.) K_0 is assumed small throughout this work so that it is possible to determine the properties of the forced motion using a simple perturbation expansion in powers of K_0. We nondimensionalize the coning frequency as follows,

$$\tau = \frac{\bar{\tau}}{(\Omega + \bar{\tau} \cos K_0)} \tag{1}$$

and we define the Reynolds number by

$$Re = \frac{(\Omega + \bar{\tau} \cos K_0)a^2}{\nu} \tag{2}$$

As a consequence of the assumption that $K_0 \ll 1$, $\cos K_0$ is replaced by unity in the above and in the following. The typical time, length, velocity, and pressure scales used to nondimensionalize the flow variables are $(\Omega + \bar{\tau})^{-1}$, a, $(\Omega + \bar{\tau})a$, and $\rho a^2(\Omega + \bar{\tau})^2$, where ρ is the density of the fluid.

In a previous paper by Hall et al.,[2] hereafter referred to as HSG, we used the spatial eigenvalue approach to determine the forced motion in the projectile at finite values of the Reynolds number. Here, we aim to extend the results of HSG to the high Reynolds number limit and show that in this case there is a significant simplification of the problem. We now indicate how the appropriate partial differential system to be solved can be derived from the Navier-Stokes equations of motion. Our derivation is, of course, only brief and so the reader is referred to HSG and the references therein for a more complete account.

First, the Navier-Stokes equations are written with respect to an inertial cylindrical coordinate system (r, θ, x) with corresponding velocity components (u, v, w) and pressure p. The coning motion of the projectile means that the boundary conditions must be applied at a moving surface; this is the main drawback in the use of the inertial reference frame, but for small angles, a Taylor series expansion of the different flow quantities about the mean position of the cylinder produces boundary conditions at a fixed surface. Thus, it is assumed that the motion of the cylinder is proportional to $\exp i\{ft - \theta\}$ where t denotes nondimensional time and f is, in general, the nondimensional complex frequency of the projectile motion. We shall take f to be real so that

$$f = \tau \tag{3}$$

Since the coning angle K_0 has been assumed small, we expect only small departures from solid-body rotation, and the velocity components are, therefore, $(-K_0u^*, r - K_0v^*, -K_0w^*)$ and the pressure is $\frac{1}{2}r^2 - K_0p^*$. Here, an asterisk denotes a perturbation quantity.

It is assumed in our calculation that the motion of the cylinder is specified; we do not allow for a feedback from the

Received March 26, 1990; revision received Jan. 27, 1991; accepted for publication Feb. 1, 1991.

*Professor of Mathematics.

†Research Scientist, Launch and Flight Division (deceased).

‡Aerospace Engineer, Launch and Flight Division. Member AIAA.

fluid to the projectile. Following HSG, it is convenient to define complex velocities and pressures, denoted here by boldfaced type and given by

$$(u^*, v^*, w^*, p^*) = \mathrm{Re}\{(\boldsymbol{u}, \boldsymbol{v}, \boldsymbol{w}, \boldsymbol{p}) \exp i\{ft - \theta\}\} \quad (4)$$

The resulting nondimensional Navier-Stokes equations are

$$i(f-1)\boldsymbol{u} - 2\boldsymbol{v} = -\boldsymbol{p}_r + Re^{-1}\left[\nabla^2\boldsymbol{u} - \frac{2}{r^2}\boldsymbol{u} + \frac{2i}{r^2}\boldsymbol{v}\right]$$

$$i(f-1)\boldsymbol{v} + 2\boldsymbol{u} = (i/r)\boldsymbol{p} + Re^{-1}\left[\nabla^2\boldsymbol{v} - \frac{2}{r^2}\boldsymbol{v} - \frac{2i}{r^2}\boldsymbol{u}\right]$$

$$i(f-1)\boldsymbol{w} = -\boldsymbol{p}_x + Re^{-1}\left[\nabla^2\boldsymbol{w} - \frac{1}{r^2}\boldsymbol{w}\right]$$

$$(r\boldsymbol{u})_r - i\boldsymbol{v} + r\boldsymbol{w}_x = 0$$

where $\nabla^2 = \partial_r^2 + (1/r)\partial_r + \partial_x^2$ and subscripts denote partial derivatives.

We now choose to seek separable solutions of these equations that take the form

$$(\boldsymbol{u}, \boldsymbol{v}, \boldsymbol{w}, \boldsymbol{p}) = [U(r)\sin Kx,\ V(r)\sin Kx,\ W(r)\cos Kx,\ P(r)\sin Kx] \quad (5)$$

and in this case it follows that (U, V, W, P) satisfies

$$[Re^{-1}(\nabla_1 - r^{-2}) - iM]U + 2[1 + (i/r^2 Re)]V - P_r = 0 \quad (6a)$$

$$[Re^{-1}(\nabla_1 - r^{-2}) - iM]V - 2[1 + (i/r^2 Re)]U + \frac{iP}{r} = 0 \quad (6b)$$

$$[Re^{-1}\nabla_1 - iM]W - KP = 0 \quad (6c)$$

$$(rU)_r - iV - KrW = 0 \quad (6d)$$

where

$$M = f - 1$$

$$\nabla_1 \equiv d_{rr} + \frac{1}{r}d_r - \left[\frac{1}{r^2} + K^2\right]$$

These equations must be solved subject to an inhomogeneous condition at $r = 1$ and an appropriate condition at $r = 0$. We obtain

$$U - iV = W = P = 0, \qquad r = 0 \quad (7)$$

at the center of the cylinder. For a discussion of the origin of Eq. (7), the reader is referred to Batchelor and Gill.[3] It suffices here to say that Eq. (7) insures that at the origin the pressure and axial velocity must be independent of the azimuthal angle, while the radial and azimuthal velocity components must vary as $\sin\theta$ there. The ordinary differential system specified by Eqs. (6), (7), and the no-slip condition at the cylinder constitutes an eigenvalue problem:

$$K = K(Re, f) \quad (8)$$

For a general discussion of eigenvalue problems of this type, see Ref. 4. Since the eigenvalue problem is of third order in K^2 and is defined on a finite interval, there are three infinite discrete spectra of eigenvalues. There is no continuous spectrum of eigenvalues.

At finite values of Re there are no real solutions of that eigenvalue problem so that solid-body rotation is stable to the first nonaxisymmetric Taylor vortex mode of instability. At infinite values of Re, solid-body rotation is, according to Rayleigh's criterion, neutrally stable and this is the origin of the real values of K that the eigenvalue problem has in the limit $Re \to \infty$. We restrict our attention to the case when the pivot point for the cylinder is midway along its axis. From Gerber et al.,[5] we know that the forced problem at small amplitudes then leads to the following conditions for $\boldsymbol{u}$, $\boldsymbol{v}$, and $\boldsymbol{w}$ at the walls:

$$\boldsymbol{u} = -i(1-f)x \quad (9a)$$

$$\boldsymbol{v} = -(1-f)x \quad (9b)$$

$$\boldsymbol{w} = i(1-f)r \quad (9c)$$

Following HSG, we transfer the inhomogeneous boundary conditions to the end wall by writing

$$\boldsymbol{u} = -i[1-f]x + u(r,x) \quad (10a)$$

$$\boldsymbol{v} = -[1-f]x + v(r,x) \quad (10b)$$

$$\boldsymbol{w} = i[1-f]r + \phi(r) + w(r,x) \quad (10c)$$

$$\boldsymbol{p} = -[1-f^2]rx + p(r,x) \quad (10d)$$

$$\phi(r) = 2if\left[r - \frac{J_1(\lambda r)}{J_1(\lambda)}\right] \quad (10e)$$

Here, J_1 denotes the order 1 Bessel function of the first type and λ is defined by

$$\lambda = (1+i)\sqrt{(1-f)Re/2} \quad (11)$$

Since we will be interested in the limit of high Reynolds numbers, we can drop the Bessel function terms in Eqs. (10) away from $r = 1$. We note in passing here that λ and, hence, $\boldsymbol{u}$, etc., have a branch cut at $f = 1$; we will not investigate such high frequencies here since the ballistic applications of our work typically correspond to values of $f < 0.5$. In terms of u, v, w, and p, it follows that the appropriate boundary conditions are

$$u - iv = w = p = 0, \qquad r = 0 \quad (12a)$$

$$u = v = w = 0, \qquad r = 1 \quad (12b)$$

$$u = v = 0, \quad w = -\phi(r) \qquad x = \pm A \quad (12c)$$

Furthermore, we note that u, v, w, and p satisfy Eqs. (5) and (6); following the spatial eigenvalue approach of HSG, we therefore write

$$u = \sum_{n=1}^{\infty} \frac{\alpha_n \sin k_n x}{\sin k_n A} u_n(r) \quad (13a)$$

$$v = \sum_{n=1}^{\infty} \frac{\alpha_n \sin k_n x}{\sin k_n A} v_n(r) \quad (13b)$$

$$w = \sum_{n=1}^{\infty} \frac{\alpha_n \cos k_n x}{\sin k_n A} w_n(r) \quad (13c)$$

$$p = \sum_{n=1}^{\infty} \frac{\alpha_n \sin k_n x}{\sin k_n A} p_n(r) \quad (13d)$$

Here, $\{k_n\}$ is the infinite sequence of eigenvalues of Eqs. (6) and (7); the coefficients $\{\alpha_n\}$ are to be determined. In HSG, these constants were found by collocation at the end walls; here we shall make the further limit $Re \to \infty$ and show how asymptotic expressions for these coefficients can be found.

II. Spatial Eigenvalue Approach in the Limit $Re \to \infty$

On the basis of our experience with the eigenvalue problem for $\{k_n\}$ at finite values of Re, we know that the eigenvalues split into groups of three that can be ordered by, for example, connecting them to the eigenvalues of a related Taylor vortex problem. We anticipate this split and therefore consider the three sets of eigenvalues $\{k_{nj}\}$, for $j = 1, 2, 3$ and $n = 1, 2, 3, \ldots$. The distribution of eigenvalues is illustrated in Fig. 1 for the case $Re = 10^3$ and $f = 0.1$; this is taken from HSG wherein the labeling of the eigenvalues is discussed. (Note that the eigenvalue $k_{3,1}$ was labeled on the basis of an analysis pertinent to the limit $Re \to 0$. However, in the limit $Re \to \infty$, it lies in the set of values determined by Stewartson's anlaysis.[6]) In Fig. 2, we show the development of the spectrum as Re increases for fixed f and $j = 1$. We note that for sufficiently small n the eigenvalues approach the real axis, whereas for large n the eigenvalues approach the imaginary axis.

On the other hand, numerical calculations in HSG showed that the $j = 2, 3$ branches had $|k_{nj}| \sim Re^{1/2}$ for $Re \gg 1$. We shall now describe the precise details of the asymptotic structure of $\{k_{nj}\}$ for $j = 1, 2, 3$ in the limit $Re \to \infty$ and, hence, put ourselves into a position to find asymptotic forms for $\{\alpha_n\}$. Splitting of the eigenvalues into triplets leads naturally to the definitions of branches 1, 2, and 3 in the complex k plane for $j = 1, 2, 3$, respectively. The corresponding amplitude functions are denoted by ε_n, γ_n, and β_n, replacing the α_n.

First, we derive the asymptotic structure of the $j = 1$ modes; the analysis is, of course, essentially inviscid and based on that given by Stewartson.[6] We seek an asymptotic solution for the nth eigenvalue k_{1n} by writing

$$k_{1n} = k_{1n}^0 + k_{1n}^1 Re^{-1/2} + k_{1n}^2 Re^{-1} + \cdots \qquad (14)$$

$$u_{1n} = u_{1n}^0 + u_{1n}^1 Re^{-1/2} + u_{2n}^2 Re^{-1} + \cdots \qquad (15)$$

together with similar expansions for v_{1n}, w_{1n}, and p_{1n}. If we define σ by

$$\sigma = i\{f - 1\}$$

then substitution of Eqs. (14) and (15) into Eqs. (6) with K replaced by k_{1n} yields a system of equations for u_{1n}^0, v_{1n}^0, w_{1n}^0, p_{1n}^0 that has the solution

$$\{\sigma^2 + 4\}u_{1n}^0 = i\left\{(1 - f)\mu_{1n}^0 J_1'(\mu_{1n}^0 r) + \frac{2J_1(\mu_{1n}^0 r)}{r}\right\} \qquad (16a)$$

$$\{\sigma^2 + 4\}v_{1n}^0 = \left\{(1 - f)\frac{J_1(\mu_{1n}^0 r)}{r} + 2\mu_{1n}^0 J_1'(\mu_{1n}^0 r)\right\} \qquad (16b)$$

$$w_{1n}^0 = \frac{-k_{1n}^0}{\sigma} J_1(\mu_{1n}^0 r) \qquad (16c)$$

$$p_{1n}^0 = J_1(\mu_{1n}^0 r) \qquad (16d)$$

$$(\mu_{1n}^0)^2 = (k_{1n}^0)^2 \frac{(3 - f)(1 + f)}{(1 - f)^2} \qquad (17)$$

The radial velocity component u_{1n}^0 in Eq. (16a) satisfies the side-wall conditions if

$$(1 - f)\mu_{1n}^0 J_1'(\mu_{1n}^0) + 2J_1(\mu_{1n}^0) = 0 \qquad (18)$$

which has an infinite number of eigenvalues on the positive real axis. Information on this spectrum can be found in Ref. 7. The eigenvalues with $j = 1$ become progressively closer to the real axis in the limit $Re \to \infty$. The Stewartson eigenvalues correspond to a choice of frequency such that $k_{1n}^0 A = \pi(1 + N)/2$ for N an even non-negative integer. Thus, at the resonant frequencies of a cylinder of given length, the $j = 1$ eigenvalues approach Stewartson's eigenvalues. Since we have not retained viscous effects in the perturbation equations, we can, of course, only make the radial velocity component vanish at $r = 1$. The other velocity components must therefore be reduced to zero within a boundary layer of thickness $Re^{-1/2}$ near $r = 1$. The determination of the velocity field within this layer will enable us to determine the order $Re^{-1/2}$ term in Eq. (14); we shall give some of the detail necessary to determine it.

We note that the perturbation equations for $r = \mathcal{O}(1)$ proceed in powers of Re so that if we define μ_{1n} by

$$\mu_{1n} = \mu_{1n}^0 + \mu_{1n}^1 Re^{-1/2} + \cdots \qquad (19)$$

then correct to order $Re^{-1/2}$, Eqs. (16) are valid if u_{1n}^0, v_{1n}^0, w_{1n}^0, p_{1n}^0, and μ_{1n}^0 are replaced by $u_{1n}^0 + u_{1n}^1 Re^{-1/2}$, etc., and then,

$$\mu_{1n}^0 \mu_{1n}^1 = k_{1n}^0 k_{1n}^1 \frac{(3 - f)(1 + f)}{(1 - f)^2} \qquad (20)$$

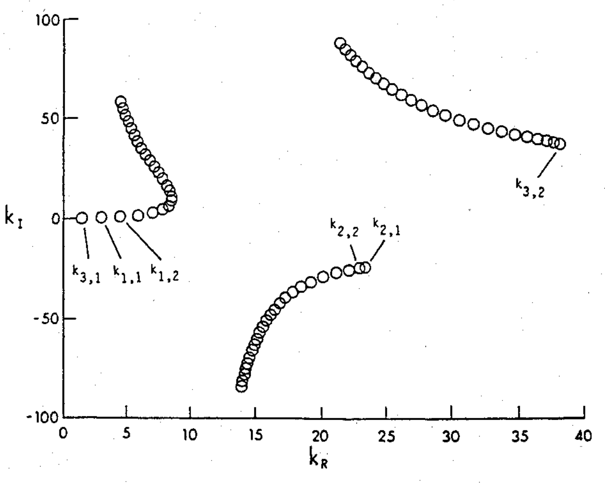

Fig. 1 First 72 eigenvalues for $Re = 10^3$, $f = 0.1$ (Ref. 2).

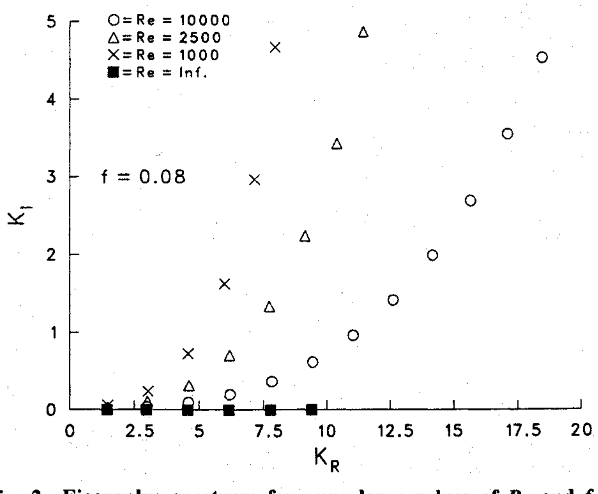

Fig. 2 Eigenvalue spectrum for some large values of Re and $f = 0.08$.

It follows that, when $r \to 1$,

$$(3 - f)(1 + f)u^1_{1n} \to -\mu^1_{1n}\, i \left\{ \mu^0_{1n} J_1(\mu^0_{1n})(1 - f) \times \left[1 + \frac{(3 - f)(1 + f)}{(\mu^0_{1n})^2 (1 - f)^2} \right] \right\} + C\zeta \tag{21}$$

where $\zeta = Re^{1/2}(1 - r)$, and C is a constant to be determined later. In the boundary layer at $r = 1$, we write

$$Re^{1/2} u_{1n} = \tilde{u}^0_{1n} + \tilde{u}^1_{1n} Re^{-1/2} + \cdots$$

together with similar expansions for v_{1n}, w_{1n}, and p_{1n}. It can be shown that the zeroth-order system obtained by substituting these expansions into Eqs. (6) written in terms of ζ yields

$$\tilde{p}^0_{1n} = \text{const}$$

$$\tilde{u}^0_{1n} = \left\{ \frac{i\tilde{p}^0_{1n}}{1 - f} \right\} \left\{ 1 + (k^0_{1n})^2 \right\} \left\{ \frac{1}{\sqrt{\sigma}} e^{-\sqrt{\sigma}\zeta} - \frac{1}{\sqrt{\sigma}} + \zeta \right\}$$

when solved subject to $\tilde{u}^0_{1n} = \tilde{v}^0_{1n} = \tilde{w}^0_{1n} = 0$, $\zeta = 0$. Thus, matching the pressure and radial velocity component when the inviscid and viscous regions meet give

$$\tilde{p}^0_{1n} = J_1(\mu^0_{1n})$$

$$\frac{iJ_1(\mu^0_{1n})[1 + (k^0_{1n})^2]}{(1 - f)\sigma^{1/2}} = \frac{i\mu^0_{1n} J_1(\mu^0_{1n})(1 - f)\mu^1_{1n}}{(3 - f)(1 + f)} \times \left\{ 1 + \frac{(3 - f)(1 + f)}{(\mu^0_{1n})^2 (1 - f)^2} \right\}$$

and an expression for C, the constant in Eq. (21). Using Eq. (20) and the eigenrelation (18), the second of the above equations can be manipulated to give

$$k_{1n} = k^0_{1n} \left\{ 1 + \frac{1 + i}{\sqrt{1 - f}\,\sqrt{2Re}} + \cdots \right\} \tag{22}$$

where k^0_{1n} is determined by Eqs. (17) and (18).

The viscous modes have an x dependence on a $Re^{-1/2}$ length scale. For convenience, we drop the $2n$ and $3n$ notation for the moment and seek a viscous eigenvalue of Eqs. (6) and (7) by writing

$$k = \sqrt{Re}\, k_0 + \frac{1}{\sqrt{Re}} k_1 + \cdots \tag{23}$$

and u, v, w, and p expand as

$$u = u_0 + \frac{1}{\sqrt{Re}} u_1 + \cdots \tag{24a}$$

$$v = v_0 + \frac{1}{\sqrt{Re}} v_1 + \cdots \tag{24b}$$

$$w = \frac{w_0}{\sqrt{Re}} + \frac{w_1}{Re} + \cdots \tag{24c}$$

$$p = \frac{p_0}{Re} + \frac{p_1}{(Re)^{3/2}} + \cdots \tag{24d}$$

The zeroth-order approximation to Eqs. (6) then yields

$$\{-k_0^2 - if + i\}u_0 + 2v_0 = 0 \tag{25a}$$

$$\{-k_0^2 - if + i\}v_0 - 2u_0 = 0 \tag{25b}$$

$$w_0 = \frac{du_0}{dr} \bigg/ k_0 \tag{25c}$$

Eqs. (25a) and (25b) are consistent if

$$k_0^2 = (3 - f)i \tag{26a}$$

or

$$k_0^2 = -(1 + f)i \tag{26b}$$

which correspond to the $j = 3$ and 2 modes, respectively. At higher order, u_0 and, hence, v_0, w_0, and p_0 are determined as solvability conditions. We find that Eqs. (26a) and (26b), respectively, lead to

$$u_0 = J_2(s_n r)$$

$$u_0 = J_0(t_n r) \tag{27a}$$

where

$$J_2(s_n) = J_0(t_n) = 0 \tag{27b}$$

A more detailed derivation of Eqs. (27) is found in HSG. Thus, Eqs. (26) correspond to two countably infinite sets of eigenvalues, and $\{s_n\}$, $\{t_n\}$ determine the order $Re^{-1/2}$ correction terms in the expansion of k. In fact, the appropriate equations are found to be

$$k_1 = \frac{-(1 - i)(4 - f)s_n^2}{2\sqrt{2}(3 - f)^3} \tag{28}$$

$$k_1 = \frac{-(2 + f)t_n^2 (1 + i)}{2\sqrt{2}(1 + f)^{3/2}} \tag{29}$$

Henceforth, we refer to the eigenvalues corresponding to Eqs. (26) using the indices $j = 3$ and 2, respectively. The structure just outlined breaks down when n is formally $\mathcal{O}(Re)$ in which case the eigenfunction has both axial and radial variations on the $Re^{-1/2}$ length scale. We can now modify the spatial eigenvalue expansions (13a–13d) using the asymptotic structure just developed; we therefore write,

$$u = \sum_1^\infty \left[\frac{\varepsilon_n i}{\{3 - f\}\{1 + f\}} \left\{ \frac{(f + 1)J_1(\mu^0_{1n} r)}{r} + (1 - f)\mu^0_{1n} J_0(\mu^0_{1n} r) \right\} \frac{\sin k^0_{1n} x}{\sin k^0_{1n} A} + \gamma_n J_0(t_n r) \frac{\sin \lambda_2 x}{\sin \lambda_2 A} + \beta_n J_2(s_n r) \frac{\sin \lambda_1 x}{\sin \lambda_1 A} \right] + \cdots \tag{30a}$$

$$v = \sum_1^\infty \left[\frac{\varepsilon_n}{\{3 - f\}\{1 + f\}} \left\{ -(1 + f) \frac{J_1(\mu^0_{1n} r)}{r} + 2\mu^0_{1n} J_0(\mu^0_{1n} r) \right\} \frac{\sin k^0_{1n} x}{\sin k^0_{1n} A} - i\gamma_n J_0(t_n r) \frac{\sin \lambda_2 x}{\sin \lambda_2 A} + i\beta_n J_2(s_n r) \frac{\sin \lambda_1 x}{\sin \lambda_1 A} \right] + \cdots \tag{30b}$$

$$w = \sum_1^\infty \frac{\varepsilon_n i k^0_{1n}}{(f - 1)} J_1(\mu^0_{1n} r) \frac{\cos k^0_{1n} x}{\sin k^0_{1n} A} + \cdots \tag{30c}$$

$$p = \sum_1^\infty \varepsilon_n J_1(\mu^0_{1n} r) \frac{\sin k^0_{1n} x}{\sin k^0_{1n} A} + \cdots \tag{30d}$$

where

$$\lambda_1 = (1 + i)\sqrt{\frac{3 - f}{2}}\sqrt{Re}$$

$$\lambda_2 = (1 - i)\sqrt{\frac{1 + f}{2}}\sqrt{Re}$$

We now apply the end-wall condition (12c) on the axial velocity component w to give

$$-2ifr = \sum_1^\infty \frac{\varepsilon_n i k_{1n}^0}{(f - 1)} J_1(\mu_{1n}^0 r) \cot k_{1n}^0 A$$

so that after multiplying both sides of the equation by $rJ_1(\mu_{1n}^0 r)$, integrating from $r = 0$ to 1 and using the well-known properties of Bessel functions we obtain

$$\varepsilon_n = \frac{4f(3 - f)\tan k_{1n}^0 A}{k_{1n}^0(\mu_{1n}^0)^2\{1 + [1/(k_{1n}^0)^2]\}J_1(\mu_{1n}^0)} \tag{31}$$

while the end-wall conditions on the radial and circumferential velocity components yield equations that can be solved for $\{\beta_n\}$ and $\{\gamma_n\}$ in terms of $\{\varepsilon_n\}$. It is at this stage that the differences between the finite and infinite Reynolds number have emerged. Thus, the amplitude functions $\{\varepsilon_n\}$, $\{\beta_n\}$, and $\{\gamma_n\}$ in the limit $Re \to \infty$ can be found explicitly using orthogonality properties of Bessel functions. At finite values of Re, HSG found it necessary to use either collocation or a least squares approach in order to find the corresponding amplitudes. At higher order in the procedure that we have just begun, the side-wall boundary layer comes into play at the end walls; at that stage, the higher order amplitude coefficients must be found by collocation or the least squares method.

It follows from Eqs. (30d) and (31) that p on the end wall, $x = A$, can be expressed as the infinite series

$$p = 4f(3 - f)\sum_1^\infty \frac{k_{1n}^0 \tan k_{1n}^0 A J_1(\mu_{1n}^0 r)}{(\mu_{1n}^0)^2 J_1(\mu_{1n}^0)[1 + (k_{1n}^0)^2]} \tag{32}$$

which is correct up to order Re^0.

Pressure Coefficient

We shall now use the high-Reynolds-number form of the spatial eigenvalue approach to find the pressure exerted by the fluid on the container. Since almost all of the available experimental results for pressure correspond to measurements made at the end wall, we shall concentrate on that situation. More precisely, we use our theory to find the amplitude of the pressure measured by a pressure transducer located at the end wall. More detail of the derivation of this pressure coefficient can be found in Gerber et al.[5]

First note that p^+, the pressure calculated from the Navier-Stokes equations, is

$$p^+ = \tfrac{1}{2}r^2 - K_0 p^*$$

in the case $K_0 \to 0$. We must now relate our calculations in an inertial frame to the frame $\tilde r$, $\tilde\theta$, $\tilde x$ used in HSG, where the $\tilde x$ axis coincides with the cylinder axis. A routine calculation based on a Taylor series expansion shows that, for example,

$$\tfrac{1}{2}r^2 = \tfrac{1}{2}\tilde r^2 - K_0 \tilde r \tilde x \cos\{ft - \tilde\theta\} + \mathcal{O}(K_0^2)$$

We now let Δp be the disturbance pressure not including the contribution from solid-body rotation. At points fixed on the surface of the cylinder

$$\Delta p = \tfrac{1}{2}r^2 - K_0 p^*(\tilde r, \tilde\theta, \tilde x, t) - \tfrac{1}{2}\tilde r^2$$

and since $p^*(\tilde r, \tilde\theta, \tilde x, t) - p^*(r, \theta, x, t) = \mathcal{O}(K_0)$ it follows that

$$\Delta p = -K_0[-p_i \sin(ft - \theta) + (p_r + rx) \times \cos(ft - \theta)] + \mathcal{O}(K_0^2)$$

Here, subscripts r and i denote the real and imaginary parts of a complex quantity. Now, since

$$\mathbf{p}_r + rx = p_r + f^2 rx, \qquad \mathbf{p}_i = p_i$$

the pressure coefficient $c_p = |\Delta p|/K_0$ may be written as

$$c_p = \sqrt{(\mathbf{p}_r + rx)^2 + \mathbf{p}_i^2} \tag{33}$$

In then follows from Eqs. (32) and (33) that c_p calculated using the spatial eigenvalue approach in the limit $Re \to \infty$ is given by

$$c_p = \left| \frac{4f(1 - f)^2}{1 + f} \sum_1^\infty \frac{\tan k_{1n}^0 A J_1(\mu_{1n}^0 r)}{k_{1n}^0(1 + k_{1n}^{0\,2})J_1(\mu_{1n}^0)} + f^2 rA \right| + \mathcal{O}(Re^{-1/2}) \tag{34}$$

Equation (34) is not uniformly valid since at the Stewartson eigenfrequencies the unperturbed state can support neutral eigenfunctions. However, it is clear that c_p will become unbounded if k_{1n}^0 corresponds to one of the Stewartson eigenvalues in which case $\tan k_{1n}^0 A = \infty$. In fact, our expansion procedure is readily modified to take account of this possibility. Suppose then that f is an eigenfrequency $\bar f$ of the inviscid problem. Without any loss of generality, we can suppose that $k_{11}^0 A = \pi/2$ so that ε_1 is formally infinite. In order to remove this singularity, we note from Eq. (31) that if higher order terms are retained then ε_1 is in fact $\mathcal{O}(R^{1/2})$ when $f = \bar f$. Since $k_{1n}^0 = k_{1n}^0(f)$ and we wish to obtain a correct zeroth-order approximation to c_p for all values of f, we must therefore modify Eq. (30) for $f - \bar f \sim \mathcal{O}(R^{-1/2})$. Thus, Eq. (34) is the correct zeroth-order approximation to c_p for $f - \bar f \gg \mathcal{O}(Re^{-1/2})$; we refer to this situation as the nonresonant case.

It follows from our calculations for the nonresonant case by taking the limit $f \to \bar f$ that ε_1, $\{\beta_n\}$, $\{\gamma_n\}$ for all n becomes formally $\mathcal{O}(Re^{+1/2})$ when $f - \bar f = \mathcal{O}(Re^{-1/2})$.

We therefore make use of the new scalings just inferred and therefore replace Eqs. (30) by

$$\begin{aligned} u = {} & \frac{i\varepsilon_1\sqrt{Re}}{(3 - f)(1 + f)}\left\{\frac{(1 + f)}{r}J_1(\mu_{11}^0 r) + (1 - f)\mu_{11}^0 J_0(\mu_{11}^0 r) + \cdots\right\}\frac{\sin k_{11}x}{\sin k_{11}A} \\ & + \sum_2^\infty \frac{\varepsilon_n i}{(3 - f)(1 + f)}\left\{\frac{1 + f}{r}J_1(\mu_{1n}^0 r) + (1 - f)\mu_{1n}^0 J_0(\mu_{1n}^0 r) + \cdots\right\}\frac{\sin k_{1n}^0 x}{\sin k_{1n}^0 A} \\ & + \sqrt{Re}\sum_1^\infty \gamma_n J_0(t_n r)\frac{\sin\lambda_2 x}{\sin\lambda_2 A} + \cdots \\ & + \sqrt{Re}\sum_1^\infty \beta_n J_2(s_n r)\frac{\sin\lambda_1 x}{\sin\lambda_1 A} + \cdots \end{aligned} \tag{35a}$$

$$v = \frac{\varepsilon_1\sqrt{Re}}{(3-f)(1+f)}\left\{-(1+f)\frac{J_1(\mu_{11}^0 r)}{r} + 2\mu_{11}^0 J_0(\mu_{11}^0) + \cdots\right\}\frac{\sin k_{11}x}{\sin k_{11}A}$$
$$+ \sum_2^\infty \frac{\varepsilon_n}{(3-f)(1+f)}\left\{\frac{-(f+1)J_1(\mu_{1n}^0 r)}{r} + 2\mu_{1n}^0 J_0(\mu_{1n}^0 r) + \cdots\right\}\frac{\sin k_{1n}^0 x}{\sin k_{1n}^0 A}$$
$$+ \sqrt{Re}\sum_1^\infty i\beta_n J_2(s_n r)\frac{\sin\lambda_1 x}{\sin\lambda_1 A} + \cdots$$
$$- \sqrt{Re}\sum_1^\infty i\gamma_n J_0(t_n r)\frac{\sin\lambda_2 x}{\sin\lambda_2 A} + \cdots \tag{35b}$$

$$w = \frac{ik_{11}^0}{(f-1)}\varepsilon_1\sqrt{Re}[J_1(\mu_{11}^0 r) + \cdots]\frac{\cos k_{11}x}{\cos k_{11}A}$$
$$+ \sum_2^\infty \frac{ik_{1n}^0}{(f-1)}\varepsilon_n[J_1(\mu_{1n}^0 r) + \cdots]\frac{\cos k_{1n}^0 x}{\sin k_{1n}^0 A}$$
$$+ \sum_1^\infty \frac{s_n\beta_n J_2'(s_n r)(1-i)}{\sqrt{3-f}\sqrt{2}}\frac{\cos\lambda_1 x}{\sin\lambda_1 A} + \cdots$$
$$+ \sum_1^\infty \frac{-\gamma_n t_n J_1(t_n r)(1+i)}{\sqrt{1+f}\sqrt{2}}\frac{\cos\lambda_2 x}{\sin\lambda_2 A} + \cdots \tag{35c}$$

$$p = \varepsilon_1\sqrt{Re}J_1(\mu_{11}^0 r)\frac{\sin k_{11}x}{\sin k_{11}A} + \mathcal{O}(1) \tag{35d}$$

We note that in Eqs. (35) f formally differs from $\bar{f}$ by $\mathcal{O}(Re^{-1/2})$. If we now apply the end-wall conditions on the radial and circumferential velocity components, we find, after using the well-known orthogonality properties of Bessel functions, that

$$\gamma_n J_1^2(t_n) = \frac{-\mu_{11}^0\,\varepsilon_1 i}{(1+f)}\int_0^1 rJ_0(\mu_{11}^0 r)J_0(t_n r)\,\mathrm{d}r \tag{36a}$$

$$\beta_n[J_2'(s_n)]^2 = \frac{-i\varepsilon_1\,\mu_{11}^0}{(3-f)}\int_0^1 rJ_2(\mu_{11}^0 r)J_2(s_n r)\,\mathrm{d}r \tag{36b}$$

The end-wall condition (12c) on the axial velocity component then gives

$$\frac{ik_{11}\varepsilon_1\sqrt{Re}}{(f-1)}J_1(\mu_{11}^0 r)\cot k_{11}A + \sum_2^\infty \frac{\varepsilon_n ik_{1n}^0}{(f-1)}J_1(\mu_{1n}^0 r)\cot k_{1n}^0 A$$
$$+ \sum_1^\infty \frac{s_n\beta_n J_2'(s_n r)(1-i)\cot\lambda_1 A}{\sqrt{2}\sqrt{3-f}} + \sum_1^\infty \frac{-\gamma_n t_n J_1(t_n r)(1+i)\cot\lambda_2 A}{\sqrt{2}\sqrt{1+f}} = -2ifr$$

We now multiply this equation by $rJ_1(\mu_{11}^0 r)$ and integrate from $r = 0$ to 1 and replace β_n and γ_n using Eqs. (36). After some manipulations, we can show that

$$\varepsilon_1\left[\frac{\sqrt{Re}}{2}\cot k_{11}A\left(1+\frac{1}{(k_{11})^2}\right)J_0^2(\mu_{11}^0)\left(\frac{f-1}{f+1}\right)^2\frac{(\mu_{11}^0)^2 ik_{11}}{f-1} - \frac{(1+i)\cot\lambda_1 A}{\sqrt{2}(3-f)^{3/2}}(\mu_{11}^0)J_0(\mu_{11}^0)S_1 - \frac{(1-i)\cot\lambda_2 A}{\sqrt{2}(1+f)^{3/2}}(\mu_{11}^0)^2 J_0^2(\mu_{11}^0)S_2\right]$$
$$= \frac{-2if}{\mu_{11}^0}J_2(\mu_{11}^0) \tag{37}$$

where

$$S_1 = \sum_1^\infty \frac{s_n z_n}{[(\mu_{11}^0)^2 - s_n^2]J_1(s_n)}$$
$$S_2 = \sum_1^\infty \frac{t_n^2}{[(\mu_{11}^0)^2 - t_n^2]^2}$$

Here

$$z_n = \int_0^1 rJ_2'(s_n r)J_1(\mu_{11}^0 r)\,\mathrm{d}r$$

We note that in Eq. (37) $\sqrt{Re}\cot k_{11}A \sim \mathcal{O}(Re^0)$ because f differs from $\bar{f}$ by $\mathcal{O}(Re^{-1/2})$. Finally, we note that $\cot\lambda_1 A$ and $\cot\lambda_2 A$ to this order can be replaced by $-i$ and $+i$, respectively. Thus, with ε_1 given by Eq. (37) the pressure perturbation is

$$p = \varepsilon_1\sqrt{Re}J_1(\mu_{11}^0 r) \tag{38}$$

which is, of course, $\mathcal{O}(Re^{1/2})$ larger than that in the nonresonant case. It can be shown from Eq. (37) that, when $1 \gg f - \bar{f} \gg Re^{-1/2}$, Eq. (38) is consistent with that obtained from Eq. (32) by taking the limit $f \to \bar{f}$. Thus, the formula

$$p = \varepsilon_1\sqrt{Re}J_1(\mu_{11}^0 r) + \sum_2^\infty \frac{4f(1-f)^2}{(1+f)}\frac{\tan k_{1n}AJ_1(\mu_{1n}^0 r)}{(k_{1n}^0)[1+(k_{1n}^0)^2]J_1(\mu_{1n}^0)} \tag{39}$$

gives a correct zeroth-order approximation to p for all f. The pressure coefficient c_p is thus given by

$$c_p = \left|\frac{4f(1-f)^2}{1+f}\sum_2^\infty \frac{\tan k_{1n}^0 AJ_1(\mu_{1n}^0 r)}{(k_{1n}^0)[1+(k_{1n}^0)^2]J_1(\mu_{1n}^0)} + f^2 rA + \varepsilon_1\sqrt{Re}J_1(\mu_{11}^0 r)\right| \tag{40}$$

with ε_1 given by Eq. (37).

We close this section with a discussion of the relationship between our resonant expansion procedure discussed earlier and the viscous correction to Stewartson's inviscid theory given by Wedemeyer.[8] In the latter paper, Wedemeyer showed how a viscous correction to the inviscid theory could be obtained by considering viscous boundary layers at the ends and side wall of the cylinder. [We observe that α and β of Eqs. (33a) and (33b) of Ref. 8 are related to λ_1 and λ_2 of Eqs. (30) of this paper as follows: $\lambda_1 = ia\alpha$, $\lambda_2 = -ia\beta$.] We note that, away from the end walls, the terms that appear inside the summations in Eqs. (35) are exponentially small. The term that remains in the expressions for the velocity and pressure corresponds to Stewartson's eigenvalue. However, the axial wave number used there is k_{11} correct to order $Re^{-1/2}$. Thus, there is a viscous correction in our expansion that arises from the fact that we choose to continue the inviscid expansion in order to take care of the viscous side-wall layer. Thus, the modified eigenfunction we have used is precisely that implied by Wedemeyer's Eq. (16).[8] At the ends of the cylinder, all of the ratios of the trigonometric functions are $\mathcal{O}(1)$, so that all of the terms are to be retained. Now, the terms proportional to $\sin(\lambda_j x)$ and $\cos(\lambda_j x)$ are needed in order to satisfy the end-wall conditions. If we choose to look at the unforced problem, then it can be shown that the effect of these terms is exactly equivalent, in a formal asymptotic sense, to Wedemeyer's conditions (18) and (19). Thus, for the unforced problem at the resonant frequency, our expansion is equivalent to Wedemeyer's. Notice, however, that the form of our expansion enables us to determine in a precise asymptotic form the forced velocity field both at the resonant frequency and elsewhere. That is not the case for Wedemeyer's theory, and so we can interpret Eqs. (35) as being a generalization of Wedemeyer's work to the forced problem at all frequencies.

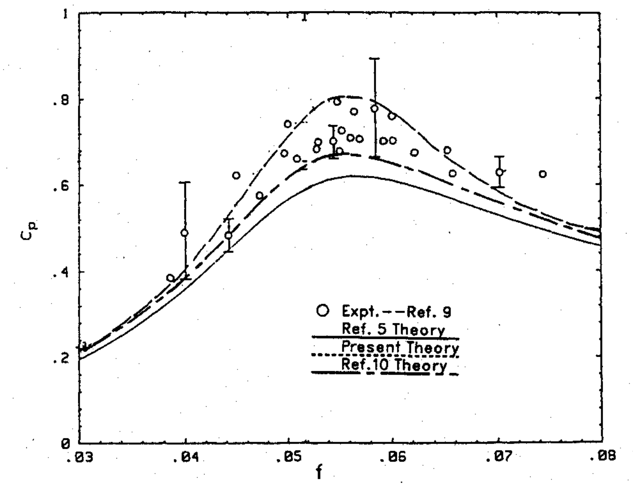

Fig. 3a Behavior of c_p calculated using the composite expansion with $A = 3.1481$, $Re = 5 \times 10^3$ (experimental points from Ref. 7).

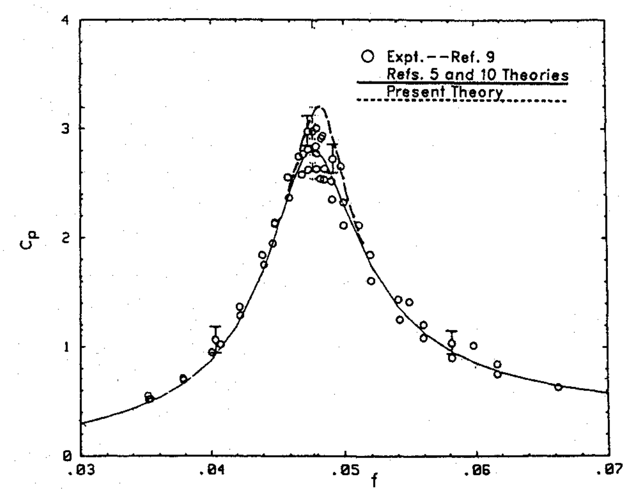

Fig. 3b Behavior of c_p calculated using the composite expansion with $A = 3.1481$, $Re = 10^5$.

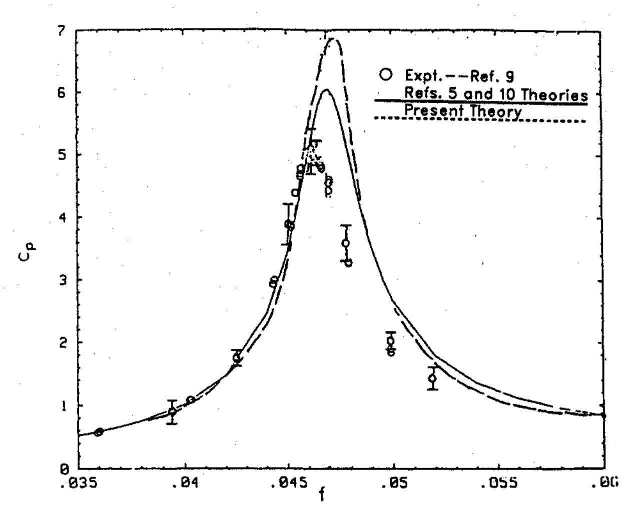

Fig. 3c Behavior of c_p calculated using the composite expansion with $A = 3.1481$, $Re = 5 \times 10^5$.

III. Results and Discussion

We shall give results only for the composite expansion (40) rather than plot separately the resonant and nonresonant expansions. In particular, we will compare our results with those of Whiting,[9] who investigated the problem experimentally. In Figs. 3a–3c, we compare with experimental data for the pressure coefficient measured at $r = 0.668$ with $A = 3.1481$ at three different values of the Reynolds number. Also shown in these figures are curves representing theoretical results from Gerber et al.[5] and Murphy.[10] Both of the latter calculations used approximate end-wall conditions obtained using Wedemeyer's approach. At $Re = 5 \times 10^3$, the results of the

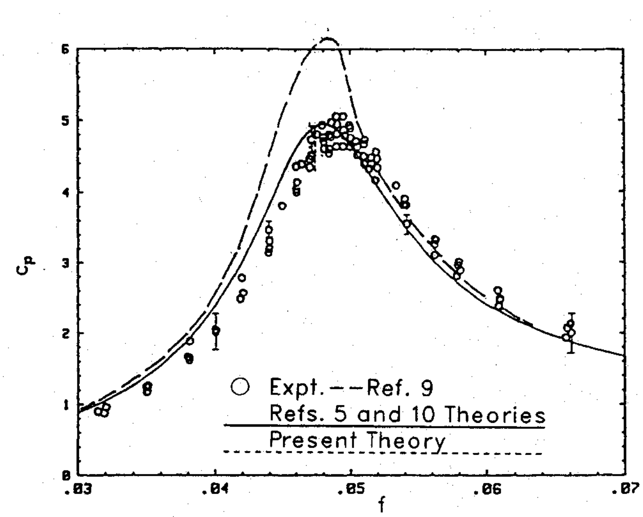

Fig. 4a Behavior of c_p calculated using the composite expansion with $A = 1.0509$, $Re = 10^5$.

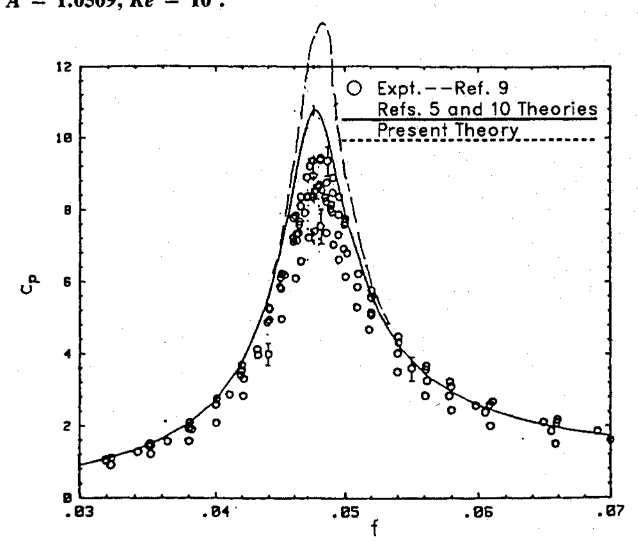

Fig. 4b Behavior of c_p calculated using the composite expansion with $A = 1.0509$, $Re = 5 \times 10^5$.

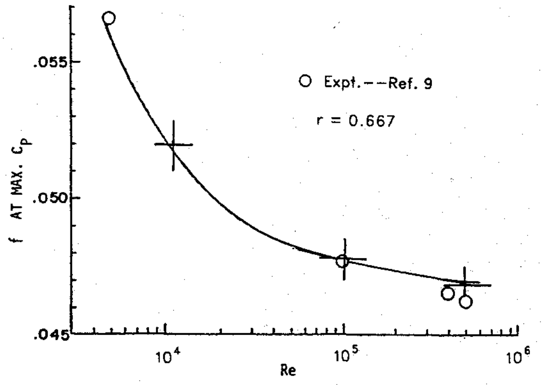

Fig. 5 Variation of the frequency of peak response with Re for A = 3.148: solid line is from the approach of Ref. 5; crosses are from the present calculations.

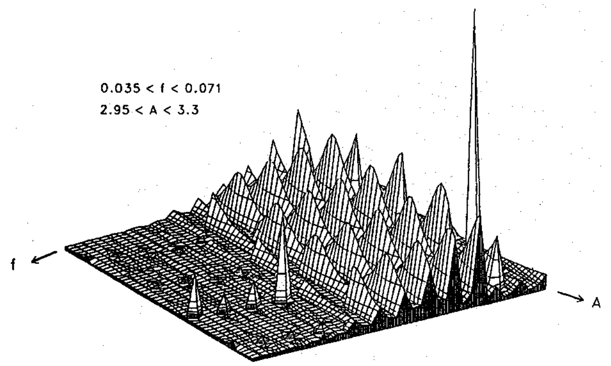

Fig. 6a Three-dimensional plot of c_p against A and f for the case $Re = 10^5$.

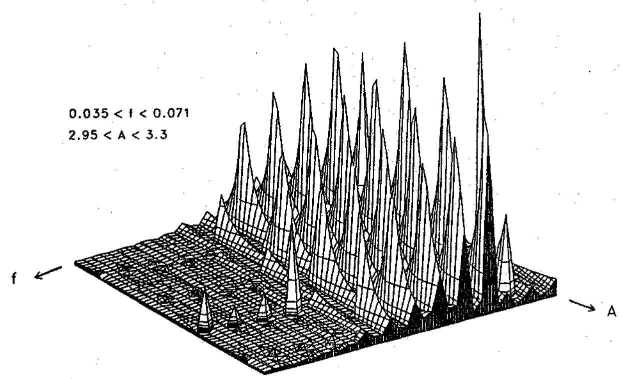

Fig. 6b Three-dimensional plot of c_p against A and f for the case $Re = 5 \times 10^5$.

present approach and Ref. 9 agree more closely with experiment than the results of Ref. 5 theory. At $Re = 10^5$, the present theory gives as good agreement with the measurements as the other approaches, but at the highest value of the Reynolds number, our theory overestimates the pressure coefficient at the resonant frequency. Apart from the immediate neighborhood of the resonant frequency, the different theoretical approaches at the two highest values of Re are in excellent agreement. The difference between the predicted resonant response and the experimental data could presumably be eliminated by proceeding with the present calculation to the next order.

In Figs. 4, we show a similar comparison at $A = 1.0509$; again we see that the differences in the two approaches are small except for a small interval near the resonant frequency. In Fig. 5, we show the variation of the resonant frequency with Reynolds number for $A = 3.1481$.

In Figs. 6, we show three-dimensional plots of the pressure coefficient at three different Reynolds numbers over a portion of the aspect ratio frequency plane. Constant intervals in f and A are used in these plots. The localized peaks correspond to resonant responses caused by the excitation of one of the Stewartson modes. Such plots are useful in picking out portions of parameter space with certain properties; more detailed plots or variations can be obtained from the program written to calculate c_p. Two points about the approach that we have developed here are in order.

1) The composite expansion is relevant whenever any one of the Stewartson eigenvalues occurs; the eigenvalue whose eigenfunction is rescaled by a factor $\sqrt{Re}$ is taken to be that eigenvalue.

2) The computational time for the present approach is trivial in comparison to that required for the different aproaches mentioned earlier. For example, all of the calculations used to supply the data for the three-dimensional plots (with 2500 nodes) were carried out in about 1 h on an Olivetti M24 PC.

References

[1]Vaughn, H. R., Oberkampf, W., and Wolfe, W. R., "Fluid Motion Inside a Spinning Nutating Cylinder," *Journal of Fluid Mechanics*, Vol. 150, 1985, pp. 121–138; also, "Numerical Solution for a Spinning, Nutating Fluid-Filled Cylinder," Sandia National Lab., Rept. 83-1789, Albuquerque, NM, Dec. 1983.

[2]Hall, P., Sedney, R., and Gerber, N., "Dynamics of the Fluid in a Spinning Coning Cylinder," *AIAA Journal*, Vol. 28, No. 5, 1990, pp. 828–835; also, "Fluid Motion in a Spinning, Coning Cylinder via Spatial Eigenfunction Expansion," U.S. Army Ballistic Research Lab., Rept. BRL-TR-2813, Aberdeen Proving Ground, MD (AD A190758), Aug. 1987.

[3]Batchelor, G. K., and Gill, A. E., "Analysis of the Stability of Axisymmetric Jets," *Journal of Fluid Mechanics*, Vol. 14, 1962, pp. 529–551.

[4]Blennerhasset, P. J., and Hall, P., "Centrifugal Instabilities of Circumferential Flow in Finite Cylinders: Linear Theory," *Proceedings of the Royal Society of London*, Vol. A-365, 1979, pp. 191–207.

[5]Gerber, N., Sedney, R., and Bartos, J. M., "Pressure Moment on a Liquid-Filled Projectile: Solid Body Rotation," U.S. Army Ballistic Research Lab., Rept. ARBRL-TR-02422, Aberdeen Proving Ground, MD (AD A120567), Oct. 1982.

[6]Stewartson, K., "On the Stability of a Spinning Top Containing Liquid," *Journal of Fluid Mechanics*, Vol. 5, Pt. 4, Sept. 1959, pp. 577–592.

[7]Carslaw, H. S., and Jaeger, J. C., *Conduction of Heat in Solids*, Oxford Univ. Press, Oxford, England, UK, 1947.

[8]Wedemeyer, E. H., "Viscous Corrections to Stewartson's Stability Criterion," U.S. Army Ballistic Research Lab., Rept. BRL R1325, Aberdeen Proving Ground, MD (AD 489687), June 1966.

[9]Whiting, R. D., "An Experimental Study of Forced Asymmetric Oscillations in a Rotating Liquid-Filled Cylinder," U.S. Army Ballistic Research Lab., Rept. ARBRL-TR-02376, Aberdeen Proving Ground, MD (AD A107948), Oct. 1981.

[10]Murphy, C. H., "Angular Motion of a Spinning Projectile with a Viscous Liquid Payload," U.S. Army Ballistic Research Lab., Mem Rept. ARBRL-MR-03194, Aberdeen Proving Ground, MD (AD A118676), Aug. 1982; also, *Journal of Guidance, Control, and Dynamics*, Vol. 6, No. 4, 1983, pp. 280–286.